Available online at www.sciencedirect.com
SCIENCE DIRECT®
Journal of Power Sources 134 (2004) 130–138
JOURNAL OF POWER SOURCES
www.elsevier.com/locate/jpowsour

Performance optimization of a battery–capacitor hybrid system

Godfrey Sikha, Branko N. Popov*

Centre for Electrochemical Engineering, Department of Chemical Engineering, University of South Carolina, Columbia, SC 29208 USA

Received 8 January 2004; accepted 30 January 2004

Available online 6 May 2004

Abstract

The effect of operating parameters such as the duty ratio, the pulse frequency and design parameters (the capacitor configuration index) on the performance of a battery/hybrid system were studied in detail. The highest value of the fractional capacity increase was observed at duty ratios of 0.2–0.3 depending on the frequency of operation. The increase of the discharge capacity of the hybrid system was limited above the maximum Eigen frequency. The hybrid system has smaller internal ohmic losses when compared to the battery. Higher power can be withdrawn from the hybrid system which has the same energy as that of the battery. However when compared on a mass basis, the Ragone plots indicated that the hybrid has lower power and energy densities.

Keywords: Battery–capacitor hybrid system; Capacitor configuration index; Eigen frequency

1. Introduction

Electrochemical capacitors (ultracapacitors) offer high power density when compared to battery systems and also have a relatively large energy density compared to conventional capacitors [1,2]. In the late 1990s they have gained considerable attention because of their extensive use in power distribution systems, electronic devices, uninterrupted power supply and hybrid vehicles. Several research attempts have been made to understand the performance of ultra capacitors with batteries and fuel cells under specific loads [3,4]. Despite the fact that lithium-ion batteries are superior to other battery systems, the performance of the Li-ion battery is greatly affected by high current discharges. Lithium-ion batteries have a high energy density of about 10^5 J/kg; however the power density is low, around 100 W/kg. As a result, the lithium-ion battery cannot respond to high power demands [5]. The addition of ultra capacitors in parallel with the battery broadens the utilization of the battery at higher rates of discharge because of the high power density of ultra capacitors ($\sim 10^6$ W/kg) [6]. Coupling of ultracapacitors is more beneficial under pulsed power loads which are frequently encountered in communication systems such as mobile phones, cellular devices and military applications.

Characterization of a lithium-ion battery with commercial super capacitors using impedance measurement were carried out by Chu and Braatz [6]. Holland et al. [7] analyzed the Ragone plots of the battery–capacitor hybrid systems in comparison with the battery alone under pulse loads. Studies were also done by Miller [8]. A theoretical analysis of the power and life of a battery–supercapacitor hybrid system based on circuit modeling was done by Dougal et al. [9].

In this work the effect of operating parameters such as the duty ratio, the pulse frequency and design parameters (the capacitor configuration index) on the performance of a commercial lithium-ion battery and battery ultracapacitor hybrid were studied in detail. The performance of the hybrid system was optimized by optimizing the fractional capacity increase as a function of the duty ratio, capacitor configuration index and pulse frequencies. Also the performance of the hybrid system and the battery system were compared under a similar set of operating parameters.

2. Experimental

A Sony US 18650 lithium-ion battery (1.5 Ah nominal capacity) and Maxwells PC 10 F ultra capacitor (2.5 V 10 F capacitance) were used in this study. The design characteristics for both the battery and the capacitor are shown in Table 1. The hybrid system in our experiments consisted of a single battery in parallel with a set of capacitors with an effective capacitance of 25 F. The capacitor configura-

* Corresponding author. Tel.: +1-803-777-7314; fax: +1-803-777-8265.
E-mail address: popov@engr.sc.edu (B.N. Popov).

0378-7753/$ – see front matter © 2004 Elsevier B.V. All rights reserved.
doi:10.1016/j.jpowsour.2004.01.054

Table 1

Parameter	Lithium-ion battery (1.5 Ah)	Ultracapacitor (10 F)
Operating voltage range (V)	2.5–4.2	0–2.5
Mass (kg)	0.0410	0.0055
Positive electrode material	$LiCoO_2$	Carbon
Negative electrode material	Carbon	Carbon
DC resistance (mΩ)	76	40

tion index, m which is defined as the ratio of the number of capacitors in parallel (n_p) to the number of capacitors in series (n_s) was fixed at 2.5. To attain this, five sets of two capacitors in series were connected in parallel to obtain a 25 F capacitance, and the two capacitors in series approximately had the voltage of the single battery. To avoid any overcharging of the battery, the capacitors were not fully charged before connecting them in parallel to the battery.

The high frequency pulse discharge of the hybrid was studied as a function of duty ratio, frequency and pulse amplitude. The hybrid system was charged to 4.2 V using a CC–CV (constant current constant voltage) protocol. A constant current of 0.7 A or $C/2$ rate was applied to charge the battery where C denotes the capacity of the hybrid system Next, the voltage was held constant at 4.2 V until the charging current tapered to 50 mA. The capacity of the hybrid system was assumed to be equivalent to the capacity of the battery since the capacitor has a low effective capacitance and does not contribute to a large extent to the overall energy to the system.

The discharge studies were performed using pulse frequencies in the range from 1 to 20 Hz. The discharge current amplitudes used for our studies were C, 2C, 3C, 4C and 5C. In this study, the goal was to compare the performance of the hybrid system to that of the battery.

The charge discharge studies were done using an Arbin Battery Cycler (BT-2000) capable of delivering high current pulses (up to 15 A) and pulse widths as low as 500 μs. Electrochemical characterization studies were done using the Solartron SI 1255 HF frequency response analyzer coupled with a Potentiostat/Galvanostat model 273 A.

3. Results and discussion

Fig. 1 shows a pulse current profile and the output voltage profile for a typical pulse load. The total time of a single pulse (T) is defined as the pulse period ($T = T_{on} + T_{off}$), where T_{on} and T_{off} represent the "on" and "off" pulse durations, respectively. The duty ratio γ is defined as ($\gamma = T_{on}/T$). The frequency, f of the pulse current is the number of pulses delivered per second ($f = 1/T$). As shown in Fig. 1, the output voltage has three main parts. The initial drop in the potential ΔV_{IR} is due to the effective internal resistance of the hybrid system. This drop is proportional to the applied discharge current. Also it is controlled by the total electronic resistance of the system. The second part is a response to the constant current part of the pulse I_{on} and the output voltage profile results from a combined polarization occurring in both, the super capacitor and the battery in the hybrid system. This potential drop is defined as a polarization drop (ΔV_P). During the T_{off}, the voltage profile regains the ΔV_{IR} drop, followed by the slow relaxation during which the potential tries to reach an equilibrium value. The increase in the potential during the T_{off} time is defined as the relaxation gain (ΔV_R). The difference in the potential

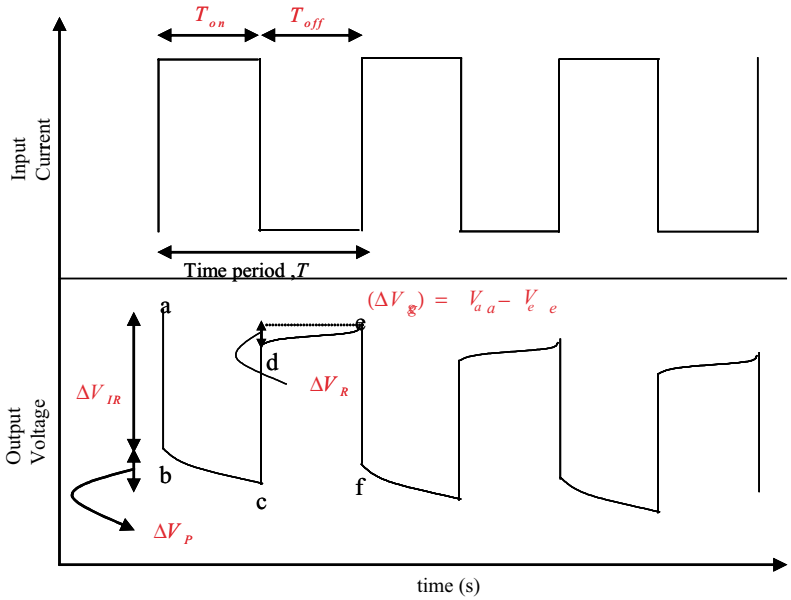

Fig. 1. A schematic of typical output voltage profile during a pulse discharge load in a battery or a hybrid system which shows the three distinct regions: the initial IR drop (a and b), the polarization drop (b and c) and the relaxation gain (d and e).

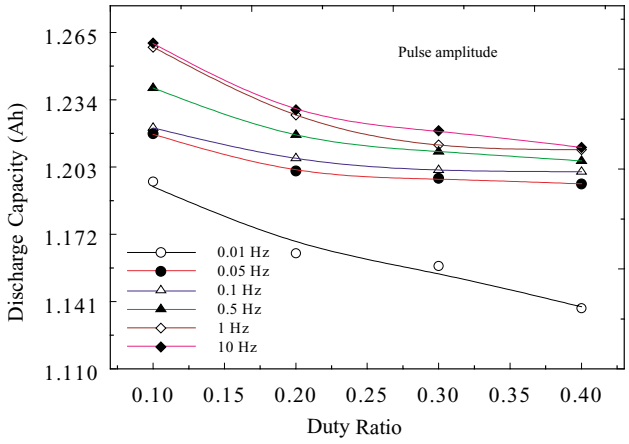

Fig. 2. Discharge capacity as a function of duty ratio for various frequencies for the battery system.

between the start of the pulse discharge (point "a" in Fig. 1) and the end of the pulse discharge (point "e" in Fig. 1) is defined as the regain potential drop (ΔV_g). In this study, the current during the T_{off} period is maintained at a very low value ($I_{off} = C/10$), which simulates the leakage current of any electronic device.

Fig. 2 shows the discharge capacity of a lithium-ion battery as a function of duty ratio for various frequencies. The pulse discharge current amplitude was fixed at 4.2 A. The markers in Fig. 2 denote the discharge capacity obtained for a specific frequency and duty ratio. It was observed that, at lower duty ratios the discharge capacity obtained is higher than that obtained at higher duty ratios for all frequencies. Also, the discharge capacity increased with the increase in the frequency of the system irrespective of the duty ratios at which the discharge was done. As shown in Fig. 2, above 1 Hz an appreciable increase in the discharge capacity was not observed.

Fig. 3 shows the discharge capacity for a hybrid system as a function of duty ratio for various frequencies. The pulse

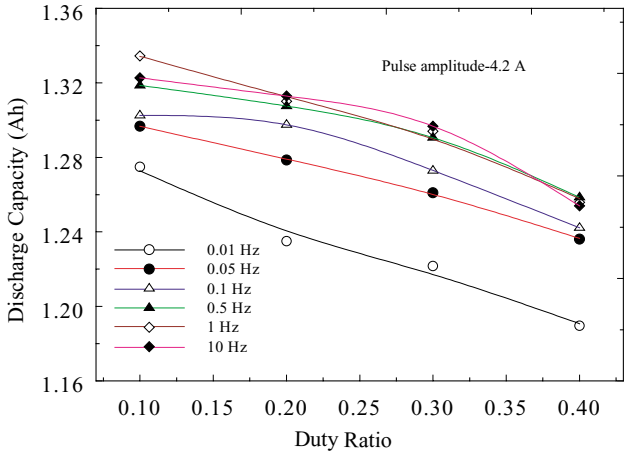

Fig. 3. Discharge capacity as a function of duty ratio for various frequencies for the hybrid system.

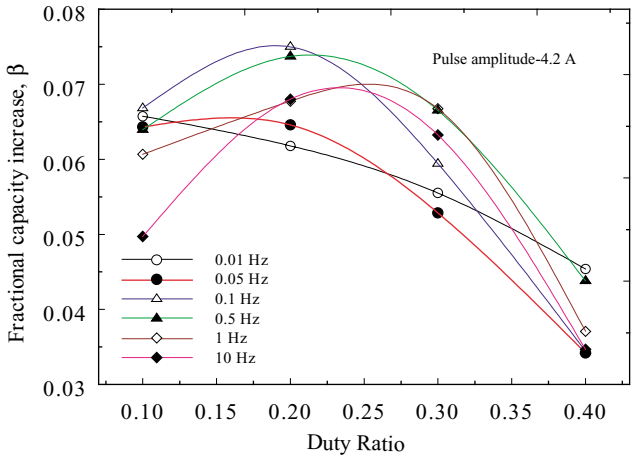

Fig. 4. Fractional capacity increase as a function of duty ratio for various frequencies.

discharge amplitude was fixed at 4.2 A. As shown in Fig. 3 the discharge capacity obtained for the hybrid system at any duty ratio or frequency is higher than that observed for the battery.

Fig. 4 shows the fractional capacity increase β as a function of duty ratio for various frequencies. The fractional capacity β is defined as the ratio of increase in the discharge capacity obtained for the hybrid system over the discharge capacity of the battery system under the same discharge protocol. As shown in Fig. 4, at lower frequencies the fractional capacity increase was maximum at low duty ratios and at higher frequencies the peak moves towards higher duty ratios. However at a duty ratio of 0.4 the fractional increase in the capacity goes to a minimum and it was found that at even higher duty ratios the fractional increase in the discharge capacity diminishes to zero. The results can be explained by taking into account the shift of the discharge curve in the case of the hybrid system observed at higher duty ratios which results in shorter run times. This phenomenon is discussed later in detail. It can also be observed that the increase of the fractional capacity levels off beyond a particular frequency. The results indicated that above 1 Hz there is not much gain in the fractional capacity. This agrees with the maximum Eigen frequency [9] given by $1/R_cC_c$ which is approximately 2.5 Hz.

Fig. 5(a)–(d) compares the discharge curves obtained for the battery and the hybrid system. The pulse discharge rate used was 4.2 A (3C) at a frequency of 1 Hz. The discharge curves were recorded at different duty ratios ranging form $\gamma = 0.1$ (Fig. 5a) to $\gamma = 0.4$ (Fig. 5d). The discharge curves indicated that irrespective of which system was investigated, the discharge capacity determined at lower duty ratios is higher than the discharge capacity obtained at higher duty ratios. As shown in Fig. 5d, the shape of the discharge profile for the hybrid system shows a distinct change at higher duty ratios ($\gamma > 0.4$) and the plateau of the hybrid system dropped low as compared to the battery and hence the increase in

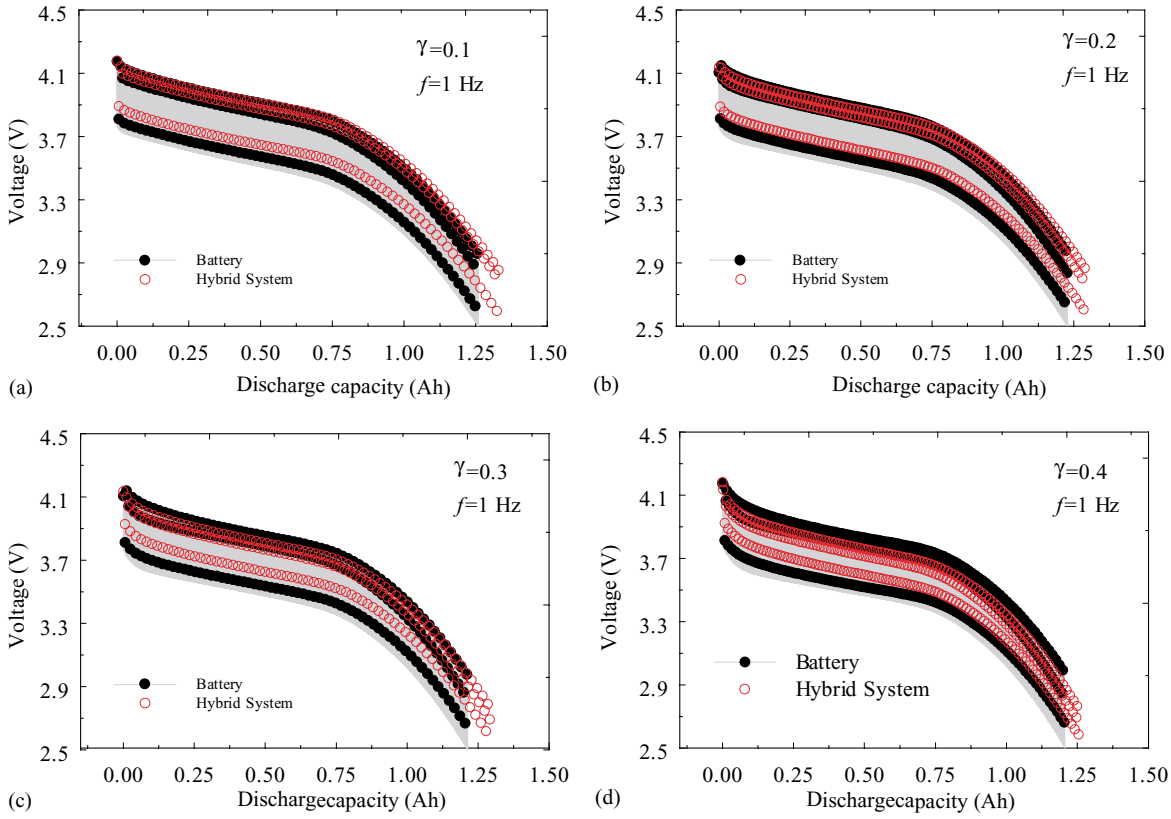

Fig. 5. Discharge curve comparison for battery and hybrid system under pulse discharge. The above discharge curves are for different duty ratios under the same pulse amplitude and frequency.

the capacity of the hybrid system over the battery was not as high as was observed at lower duty ratios.

To understand the performance of the hybrid system better, the battery and the hybrid discharge capacity were studied as a function of the IR drop (ΔV_{IR}), the polarization drop (ΔV_P) and the relaxation gain (ΔV_R).

3.1. Effect of the ohmic resistance (ΔV_{IR})

The observed increase in the discharge capacity of the hybrid system discussed above is due to a decrease in the effective resistance of the hybrid system when compared to the battery resistance. The effective resistances estimated for the battery and for the hybrid system are shown in Fig. 6. The DC resistances were estimated by discharging the battery and the hybrid by using a pulse discharge amplitude of 4.2 A, frequency, $f = 1$ Hz and a duty ratio γ of 0.4. The resistances were calculated throughout the discharge by calculating the voltage drop resulting from each current pulse. The results clearly show that a lesser value of ohmic resistance is observed for the hybrid system. The average ohmic resistance of the battery system was approximately 75 mΩ, compared to the average resistance of the hybrid system of 40 mΩ. This phenomenon can be explained by taking into account that only a fraction of the output current enters the battery (high resistance component), while the major portion of the current passes through the capacitor, while in the case of a pure battery system the complete output load is withdrawn from the battery. As a result of this decreased ohmic drop, apart from the increase in discharge capacity, the utilization of the battery is more effective in the hybrid system.

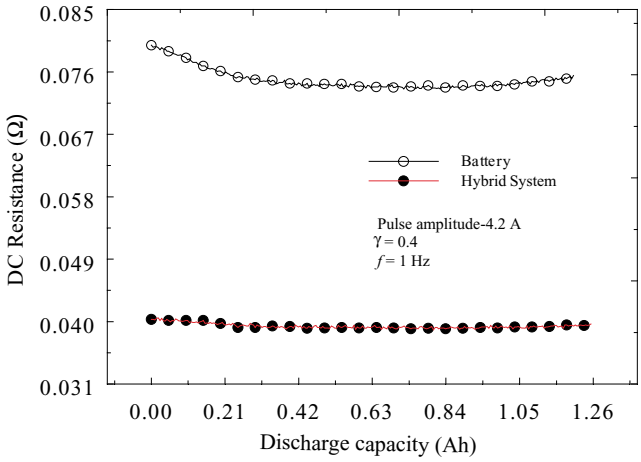

Fig. 6. Comparison of the effective resistances for battery and hybrid systems.

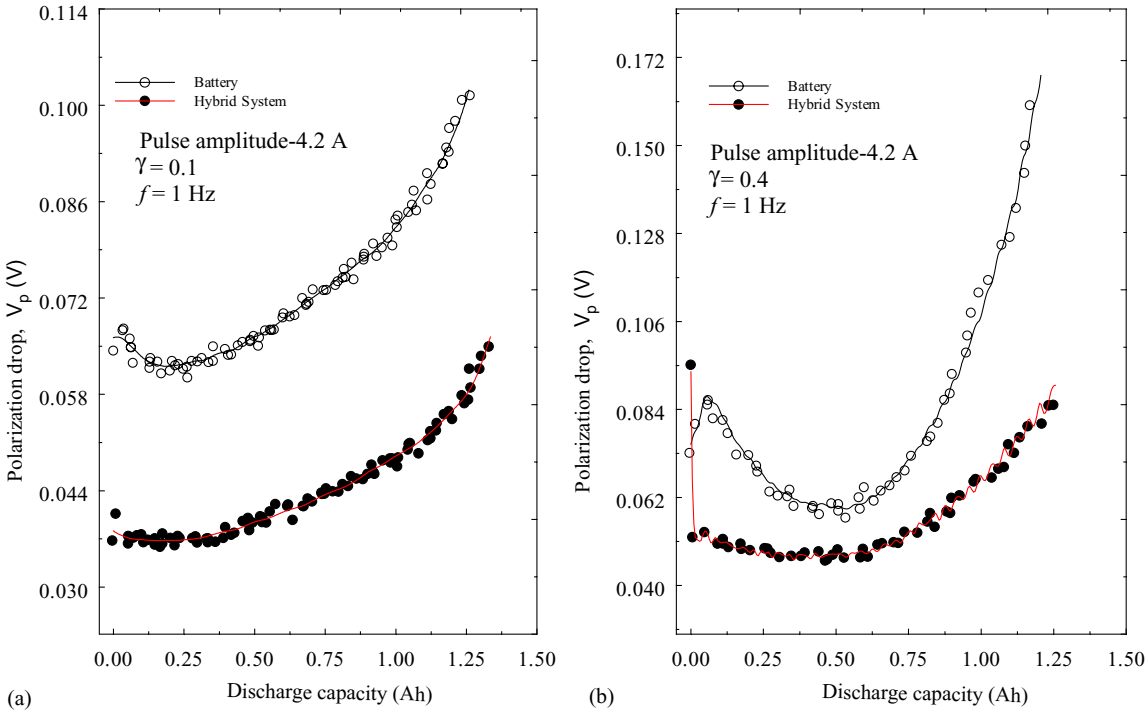

Fig. 7. Comparison of the polarization drop for battery and hybrid systems.

3.2. Effect of polarization drop (ΔV_P)

Fig. 7(a)–(b) shows the effect of the polarization drop for both the battery and hybrid systems as a function of discharge capacity. Both systems were discharged using a pulse current of 4.2 A, frequency $f = 1$ Hz and a duty ratio of $\gamma = 0.1$. The values of the polarization drop are smaller for the hybrid system when compared to the battery because of the lower currents that pass through the battery when it is part of the hybrid system. It should be noted that the output discharge profile is determined predominantly by the discharge of the battery.

As seen in Fig. 7b, at higher duty ratios ($\gamma = 0.4$), the polarization drop profile of the battery is similar to the discharge profile under high discharge rates. However, the polarization drop profile of the hybrid system is quite different. Initially the polarization drop is large, levels off at approximately 50% of discharge capacity and finally it increases as the discharge curve reaches the cut-off value. The initial large drop in the polarization potential results from a combined polarization of the battery and the capacitor. The voltage drop also increases because of the smaller (T_{off}) time of the pulse, where in the hybrid system receives the next pulse before actually reaching the equilibrium state during the off time of the previous pulse. This causes the lowering of the voltage profiles at high duty ratios. The large increase of the polarization drop in Fig. 7b, explains the observed decrease in the fractional capacity at higher duty ratios.

3.3. Effect of regain potential drop (ΔV_R)

To analyze further, the regain potential (ΔV_g) drop was calculated throughout the discharge at low and high duty ratios for both the battery and the hybrid system. This parameter gives information about how far the system reverts back to equilibrium between the start of the ‘on’ time of the pulse and the end of the corresponding ‘off’ time. In other words, it represents a difference between the potential at start of the ‘on’ time of the pulse and the end of the corresponding ‘off’ time. Due to the fact that the relaxation times of the capacitor and the battery are different, the duty ratio used to discharge the hybrid becomes a crucial factor in controlling the value of the regain potential drop.

Fig. 8(a)–(b) compares the regain potential drop between the battery and the hybrid system at duty ratio of 0.1 and 0.4, respectively. The same frequency and current amplitude were used to discharge both systems. A higher drop in the regain potential is observed in the case when the hybrid system is discharged at high duty ratios. This is probably due to the fact that initially during the high polarization drop the hybrid system requires longer pulse ‘off’ time to restore the system completely to equilibrium. Since the relaxation times are smaller, the next pulse is delivered before a complete equilibrium is established. This phenomenon causes a shift in the voltage profile as a result of which the voltage reaches the cut-off value quickly. This also explains the observed smaller fractional increase in capacity at higher duty ratios in Fig. 4.

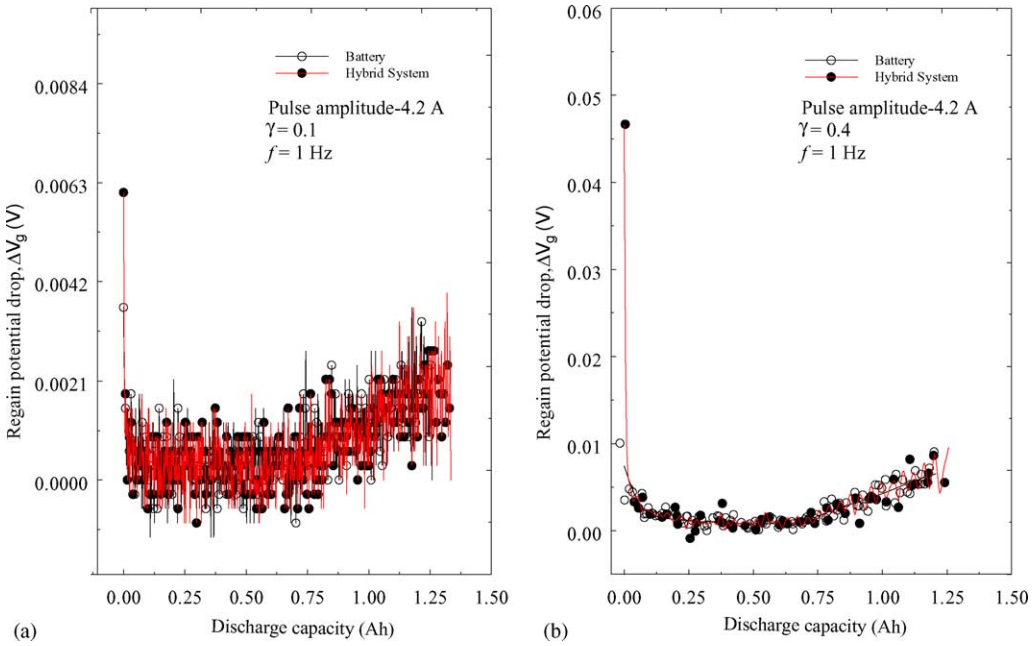

Fig. 8. Comparison of the polarization drop for battery and hybrid systems. The above plot is for a pulse discharge at a pulse amplitude of 4.2 A with frequency, $f = 1$ Hz and duty ratio $\gamma = 0.4$.

Initially, the drop in the regain potential for the battery system is smaller when compared to the drop observed for the hybrid system which suggests that the battery quickly reverts backs to equilibrium potential even at short relaxation times. This phenomenon also occurs at lower duty ratio. However, the values of the drop in the regain potential at low duty ratios are relatively small and hence the voltage profile is not affected strongly. This is in agreement with the results presented in Fig. 5(a)–(d) where there is a significant drop in the discharge plateau at high duty ratio ($\gamma = 0.4$) while at low duty ratios the discharge curves closely overlaps.

Figs. 9 and 10 shows the variation of the energy with duty ratio at various frequencies. The pulse discharge amplitude was fixed at 4.2 A. The markers denote the discharge energy estimated at specified duty ratios. The total energy of a series of pulses during the discharge was calculated from the formula

$$E_t = \int_0^t v(t)i(t)\,\mathrm{d}t = \sum_{i=1\&t=0}^{i=\tau/d_\mathrm{p}\&t=\tau} d_\mathrm{p} f \sum_{j=1\&t=o}^{j=n\&t=T} v(t)I(t) \qquad (1)$$

where τ is the discharge time, d_p the data logging time and n the number of data points on each pulse while f and T denote the frequency and the time period of the pulse, respectively. Similar to the discharge capacity profile the discharge energy has a maximum value at lower duty ratios. It becomes smaller at higher duty ratios. This applies for the battery as well as for the hybrid system. However in the

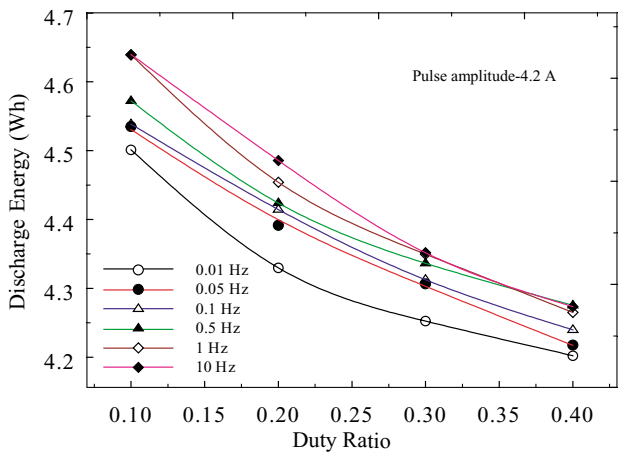

Fig. 9. Discharge energy as a function of duty ratio for various frequencies for the battery system.

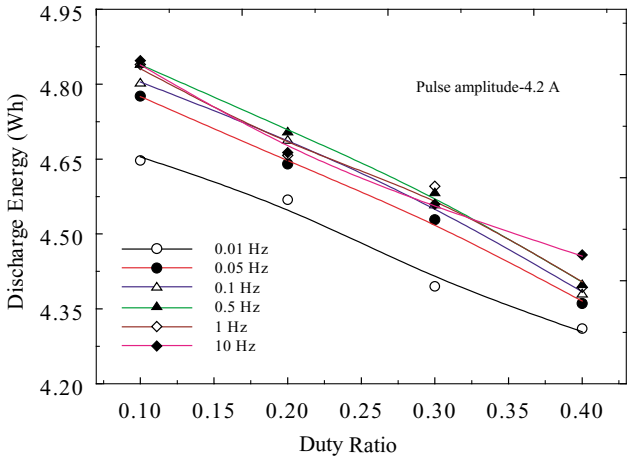

Fig. 10. Discharge energy as a function of duty ratio for various frequencies for the hybrid system.

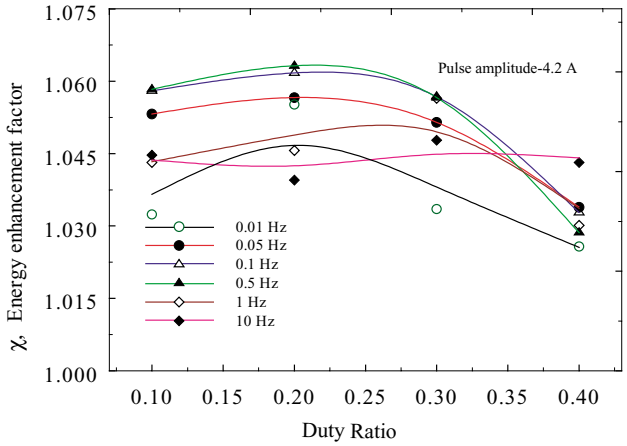

Fig. 11. Energy enhancement factor as a function of duty ratio for various frequencies.

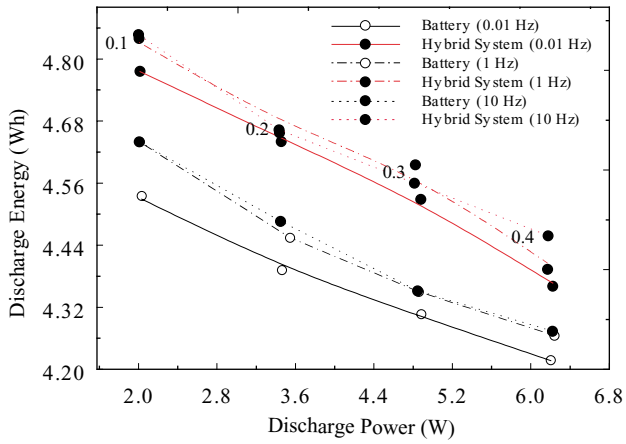

Fig. 12. Energy vs. power relationship for the battery and hybrid system.

case of the hybrid system the energy drops at a faster rate towards higher duty ratios than for the battery system. This is in agreement with the observed higher voltage drop of the hybrid system at high duty ratios which makes the product between the current and the voltage to be smaller. As shown in Figs. 9 and 10, the energy also increases with increase in the frequency until a certain value of the frequency is reached (∼1 Hz). Beyond this value, the increase in the energy levels off at all duty ratios.

Fig. 11 shows the energy enhancement factor χ as a function of duty ratio at various frequencies. The energy enhancement factor, χ is defined as the ratio of the energy obtained in the hybrid system to the energy obtained in the battery. As shown in Fig. 11, χ has a maximum value at a duty ratio of around 0.2. The explanation for the decrease in the fractional increase in capacity at higher duty ratios can be extended to the decrease in the energy enhancement factor too.

The energy versus power relationship for the battery and hybrid system is shown in Fig. 12 for different frequencies. The markers denote the energy and the average power calculated from a complete discharge at a specific duty ratio and frequency. The same pulse discharge current amplitude of 4.2 A was used to discharge both systems. The average power is calculated by using the formula:

$$P = \frac{E_t}{\tau} \quad (2)$$

The data presented in Fig. 12, indicated that the average power obtained in a hybrid system is higher for all range of frequencies. This is the other advantage of the hybrid system apart from the increase in the utilization of the battery. Fig. 12 also shows the energy–power relationship as a

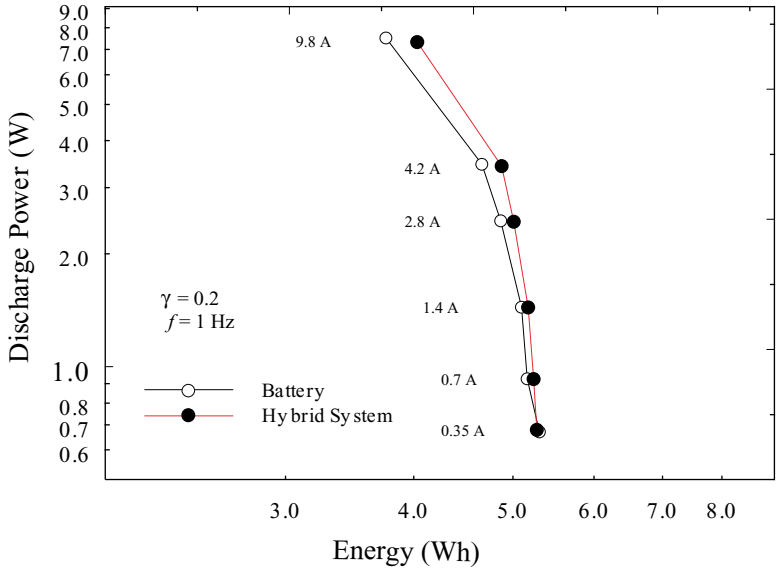

Fig. 13. Energy vs. power relationship at various pulse discharge amplitudes. The markers denote the energy and average power calculated from a complete discharge curve at a particular pulse discharge rate as denoted.

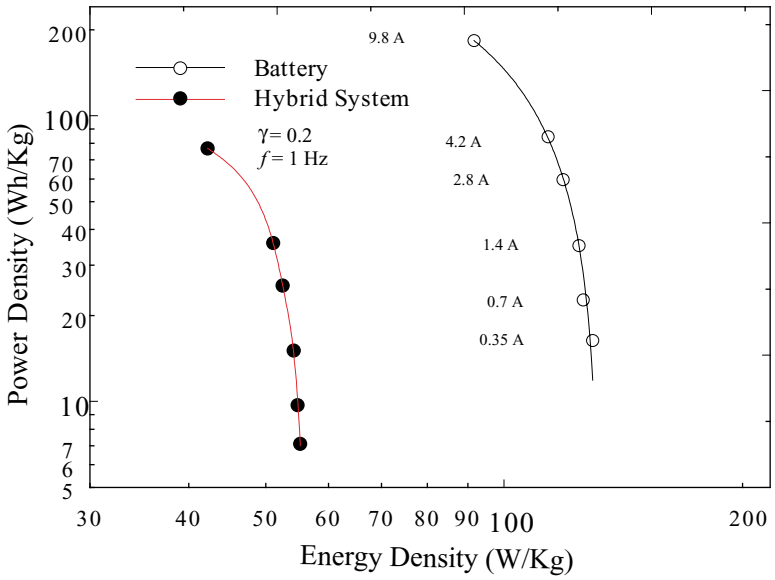

Fig. 14. Ragone plot showing the specific energy specific power relationship. The markers denote the energy and average power calculated from a complete discharge curve at a particular pulse discharge rate as denoted.

function of duty ratio for different frequencies. The average power increases with the increase in frequency. At higher values of frequencies, the energy–power relationship has a constant profile.

Fig. 13 compares the power versus energy relationship between battery and the hybrid system at a constant duty ratio and frequency for various pulse discharge amplitudes on a logarithmic scale. The markers denote the energy and the average power estimated form a complete discharge curve at a particular discharge rate which is denoted in figure. At low pulse discharge rates, the average power increased sharply with a decrease in the energy. At high pulse discharge rates, the average power increase shows smaller slope with the attained energy.

The above energy–power relationship is shown on a unit mass basis (Ragone plot) in Fig. 14. The markers denote the energy and average power calculated from a complete discharge curve at a particular discharge rate. Fig. 14 indicates a poor performance of the hybrid system in comparison with the battery on a per mass basis.

3.4. Effect of capacitor configuration index (m)

Increasing the capacitance of the capacitor network by paralleling the ultracapacitors decreases the effective resistance while increasing the voltage at a constant capacitance when the capacitors are in series increases the resistance. As defined earlier, the capacitor configuration index, m is the ratio of the number of capacitors in parallel to the number of capacitors in series. Fig. 15 shows the relationship between the capacitor configuration index and the fractional capacity increase and fractional energy increase. The plot

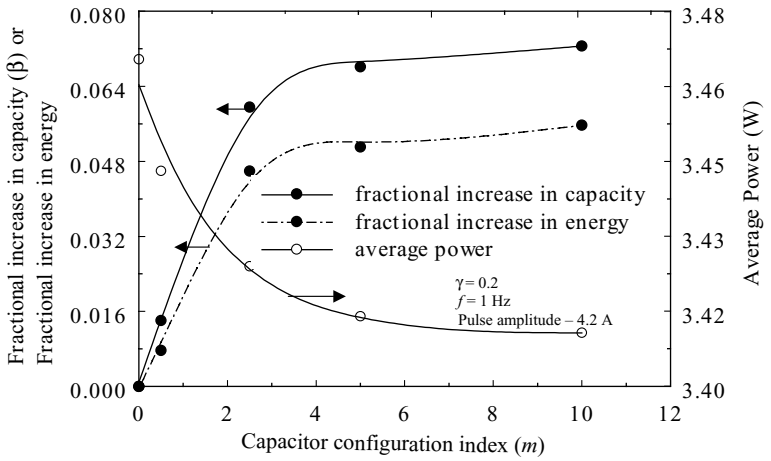

Fig. 15. Plots showing the fractional increase in the capacity and the fractional increase in energy on the left axis as a function of the capacitor configuration index. The plot corresponding to the right axis shows the average power withdrawn from the system for various capacitor configuration indices.

corresponding to the right axis shows the average power withdrawn from the system for various capacitor configuration indices. The experiments were performed at a duty ratio $\gamma = 0.2$ and a frequency $f = 1$ Hz with a pulse discharge of 4.2 A corresponding to a maximum power and utilization. The factor m was varied between 0 and 10. The value of the fractional capacity increase rises up sharply with increase in the capacitor configuration index and then saturates beyond a certain value. The maximum increase in the capacity was found to be approximately 7.2%. The fractional energy increase also followed a similar profile but starts to saturate at lower values. This is due to the fact that the discharge curve of the capacitor plays an important role in determining the overall discharge curve of the hybrid system at high values of the capacitor configuration index. This may result in the shift of the output voltage profile and in a smaller energy output. Fig. 15 also shows a decrease in the average power of the hybrid system with the increase in the capacitor configuration index for the same set of experimental conditions.

4. Optimization

The optimization of the operating conditions for a given system is based mainly on the application requirements. Some of the predominant features which most applications entail are: high power output, longer discharge period and a complete utilization of the active material. According to these studies in a case where higher discharge capacity is expected from the system, the hybrid system is obviously a better choice over the battery. The number of capacitors in parallel with the battery or the configuration index m is the next parameter to be adjusted. The fractional capacity increase is very small between $m = 5$ and 10 however, the mass of the capacitor network is doubled for these configurations. Thus, it would be better to chose a capacitor network that would match with the battery voltage and with $m = 5$.

The highest value of the hybrid fractional capacity is observed at duty ratios of 0.2–0.3 depending on the frequency of operation. The pulse frequency as observed in Fig. 4 is optimized in the range between 1 and 10 Hz. Although the system can yield slightly higher capacity at higher frequencies it would be advisable to operate at the limiting frequency (∼10 Hz) in order to avoid the use of a robust hardware power sources to deliver high frequency pulses. The Ragone plots indicated that despite many obvious advantages for light weighted applications it is disadvantageous to use a hybrid system. Similar optimization of operating conditions and design parameters for high power or energy requirements can be made from the presented experimental data.

5. Conclusion

The effect of operating parameters such as the duty ratio, the pulse frequency and design parameters (the capacitor configuration index) were studied in detail and optimized for various criteria. The incorporation of an ultracapacitor to the battery increases the run time of the battery but only at the expense of the increased weight of the system. Based on the above study an optimized discharge profile can be designed to suit the desired application. Ultracapacitors with higher power densities would be beneficial in the improvement of the Ragone plots of the hybrid system.

References

[1] B.E. Conway, Electrochemical Supercapacitors: Scientific fundamentals and Technological applications, Kluwer–Plenum, New York, 1999.
[2] R. Kotz, M. Carlen, Electrochim. Acta 45 (2002) 2483.
[3] J.R. Miller, in: Proceedings of the Fifth International Seminar on Double Layer Capacitor and Similar Energy Storage Devices, Boca Raton, FL, 4–6 December 1995.
[4] T. Atwater, P.J. Cygan, F.C. Leung, J. Power Sources 91 (2000) 27.
[5] T. Christen, M.W. Carlen, J. Power Sources 91 (2000) 210.
[6] A. Chu, P. Braatz, J. Power Sources 112 (2002) 236.
[7] C.E. Holland, J.W. Weidener, R.A. Dougal, R.E. White, J. Power Sources 109 (2002) 32.
[8] J.R. Miller, Proc. Electrochem. Soc. Conf. 95–29 (1995) 246.
[9] R.A. Dougal, S. Liu, R.E. White, IEEE Trans. Comp. 25 (1) (2002) 120.